

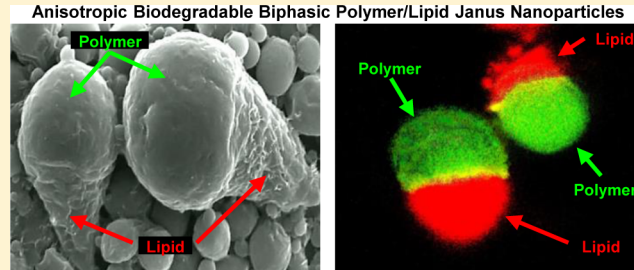
## Biodegradable Janus Nanoparticles for Local Pulmonary Delivery of Hydrophilic and Hydrophobic Molecules to the Lungs

Olga B. Garбуzenko,<sup>†,§</sup> Jennifer Winkler,<sup>‡,§</sup> M. Silvina Tomassone,<sup>\*,‡</sup> and Tamara Minko<sup>\*,†</sup>

<sup>†</sup>Department of Pharmaceutics, Rutgers, The State University of New Jersey University, 160 Frelinghuysen Rd., Piscataway, New Jersey 08854, United States

<sup>‡</sup>Department of Chemical and Biochemical Engineering, Rutgers, The State University of New Jersey, 98 Brett Road, Piscataway, New Jersey 08854, United States

**ABSTRACT:** The aim of the present work is to synthesize, characterize, and test self-assembled anisotropic or Janus particles designed to load anticancer drugs for lung cancer treatment by inhalation. The particles were synthesized using binary mixtures of biodegradable and biocompatible materials. The particles did not demonstrate cytotoxic and genotoxic effects. Janus particles were internalized by cancer cells and accumulated both in the cytoplasm and nuclei. After inhalation delivery, nanoparticles accumulated preferentially in the lungs of mice and retained there for at least 24 h. Two drugs or other biologically active components with substantially different aqueous solubility can be simultaneously loaded in two-phases (polymer-lipid) of these nanoparticles. In the present proof-of-concept investigation, the particles were loaded with two anticancer drugs: doxorubicin and curcumin as model anticancer drugs with relatively high and low aqueous solubility, respectively. However, there are no obstacles for loading any hydrophobic or hydrophilic chemical agents. Nanoparticles with dual load were used for their local inhalation delivery directly to the lungs of mice with orthotopic model of human lung cancer. *In vivo* experiments showed that the selected nanoparticles with two anticancer drugs with different mechanisms of action prevented progression of lung tumors. It should be stressed that anticancer effects of the combined treatment with two anticancer drugs loaded in the same nanoparticle significantly exceeded the effect of either drug loaded in similar nanoparticles alone.



### INTRODUCTION

Nanomedicine has been a growing branch of conventional medicine within the past decade. The variety of nanocarriers were developed and investigated for their medical applications including lipid-based formulations (liposomes, micelles, solid-lipid nanoparticles, etc.), and nonlipid-based formulations (dendrimers, mesoporous silica nanoparticles, etc.).<sup>1–11</sup> The diversity of shapes, sizes, and composition of nanoparticles allows for selecting the best suitable delivery vehicle for a specific application. For example, liposomes, self-assembled lipid vesicles have been successfully used for the delivery of different water-soluble therapeutic agents.<sup>10,12,13</sup> Micelles are typically used for the delivery of water-insoluble drugs carried because of their hydrophobic core.<sup>14–17</sup> Dendrimers, with a well-defined, regularly branched symmetrical structure and a high density of functional end groups at their periphery, have been used for the design of complex multifunctional drug delivery systems.<sup>18–21</sup> Mesoporous silica nanoparticles (MSNs) could also serve as suitable candidates for encapsulation and release of a variety of active pharmaceuticals due to their unique characteristics including a large surface area and high as well as uniform porosity.<sup>22,23</sup> Recently, a promising new type of anisotropic nanoparticles—“Janus” particles—have been discovered and synthesized. These particles exhibited enormous potential as a drug delivery system due to their dual

functionality and anisotropic nature.<sup>24,25</sup> The beauty of these particles is that they can encapsulate in one complex system both hydrophobic and hydrophilic biologically active molecules. The encapsulation of dissimilar drugs into a two compartmental single particle allows for simultaneous delivery and release at the target site, thus avoiding problems with pharmacokinetics. Current technologies enable codelivery of two hydrophobic or two hydrophilic drugs, but generally not both. Anisotropic particles offer many additional advantages such as a larger surface area to volume ratio for optimizing targeting ligand and protective coating, the ability to incorporate imaging agents in a separate compartment to enable real-time tracking of treatment, and segregation of the active payloads. Their diverse shapes, sizes, and surfaces may represent additional advantages and offer a desired pharmacokinetics, body distribution, and pharmacodynamics.<sup>26</sup> It has also been shown that particles with complex local geometries are capable of preventing initial contact with incoming macrophages, thereby evading fast clearance by the reticuloendothelial system.<sup>27</sup>

For the past decade, our research group focused on the design, development, and application of different nanocarriers

Received: June 3, 2014

Revised: October 4, 2014

Published: October 9, 2014

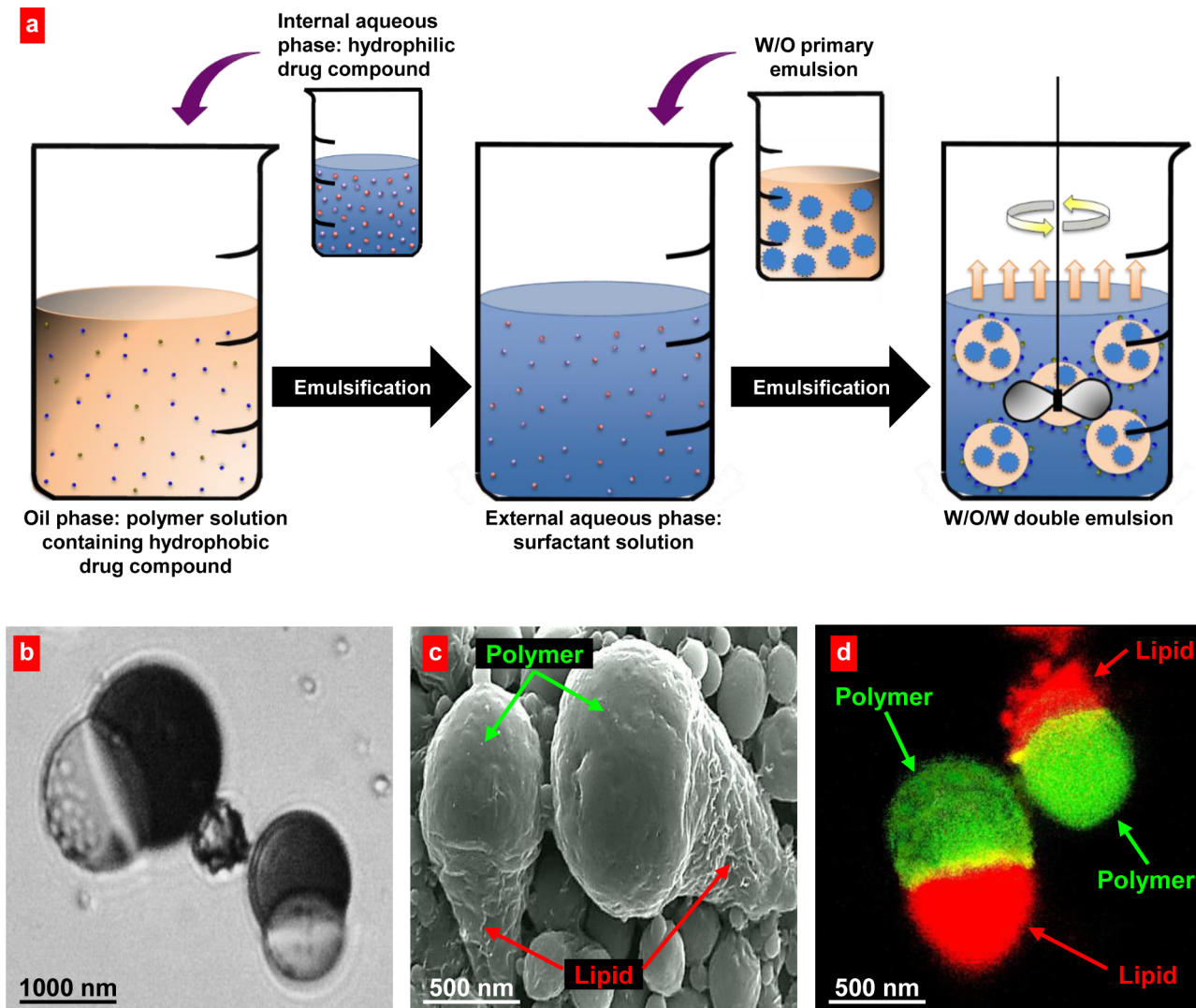


**Figure 1.** Anisotropic biodegradable biphasic polymer/lipid Janus nanoparticles. (a) Schematic of the formation process of PLGA/Precirol Janus particles: (1) Internal aqueous phase containing the hydrophilic drug is emulsified in the oil phase containing the hydrophobic drug and immiscible polymer/lipid species; (2) The primary W/O emulsion is emulsified in aqueous surfactant solution; (3) Solvent evaporation induces phase separation of the polymer and lipid, resulting in bicompartimental Janus particles. (b–d) Representative optical (b), scanning electron (c), and fluorescence (d) microscope images are shown. (b) Oil droplets in the later stages of DCM evaporation showing phase separation of PLGA-curcumin and Precirol-DOX during particle formation; (c) Polymer/lipid combinations yielded “ice cream cone” shaped particles. (d) Polymeric phase of nanoparticles was labeled with FITC (green fluorescence); and lipid phase was labeled with DiR (red fluorescence).

for the inhalation or intravenous delivery of hydrophilic and hydrophobic drugs for the efficient treatment of various diseases including several lung pathologies.<sup>10,11,23</sup> In terms of local inhalation delivery of therapeutics to the lungs, we found that the use of an appropriate nanocarrier can help to distribute the biologically active agents (drugs, nucleic acids, etc.) to the lungs and extend their retention period. This, in turn, can enhance the efficacy of the treatment and prevent possible adverse side effects upon healthy organs and tissues.<sup>10,11,23</sup>

We hypothesized that local delivery of several anticancer drugs with different aqueous solubility and mechanisms of action compartmentalized in Janus particles can provide their efficient delivery directly into the lungs, thus increase their accumulation in targeted cells and reduce adverse side effects on healthy organs by limiting drug concentration in the blood and healthy tissues. The present work was aimed at testing the hypothesis.

## MATERIALS AND METHODS

**Materials.** Dichloromethane (DCM), Poly(lactic-co-glycolic acid) (PLGA) (MW 40 000–75 000; 65:35 lactic acid: glycolic acid), surfactants poly(vinyl alcohol) (PVA), sodium dodecyl sulfate (SDS), sodium dodecyl benzylsulfate (SDBS), phosphate buffered saline (PBS), Twin 20, *N*-hydroxysuccinimide (NHS), *N*-(3-(Dimethylamino)propyl)-*N'*-ethylcarbodiimide, Ethylmethanesulfonate (EMC), doxorubicin (DOX), curcumin (CUR), fluorescein isothiocyanate (FITC), and 4',6-Diamidino-2-phenylindole dihydrochloride (DAPI) were purchased from Sigma-Aldrich (St. Louis, MO); The lipid, Precirol ATO 5 (glycerol distearate type I EP), was obtained from Gattefossé SAS (Saint-Priest Cedex, France); the near-infrared lipophilic dye, 1,1'-dioctadecyl-3,3,3',3'-tetramethylindotricarbocyanine iodide (DiR), was purchased from Invitrogen, Inc. (Grand Island, NY).

**Cell Line.** A549 human lung adenocarcinoma cells and A549 cells transfected with luciferase were obtained from the ATCC (Manassas, VA) and from Xenogen Bioscience, (Cranbury, NJ), respectively. Cells were cultured in RPMI 1640 medium (Sigma, St. Louis, MO)

supplemented with 20% fetal bovine serum (Fisher Chemicals, Fairlawn, NJ) and 1.2 mL/100 mL penicillin-streptomycin (Sigma, St. Louis, MO). Cells were grown at 37 °C in a humidified atmosphere of 5% CO<sub>2</sub> (v/v) in air. All experiments were performed on cells in the exponential growth phase.

**Synthesis of Janus Particles and Loading with Drugs.** For the in vitro and in vivo studies, Janus nanoparticles containing DOX and CUR were synthesized using a modified water-in-oil-in-water double emulsion solvent evaporation technique as previously described (Figure 1a).<sup>25,28</sup> Briefly, 25 mg DOX were dissolved in 2 mL DI water to form the internal water phase. The oil phase consisted of 2.5% w/v polymer (PLGA) and lipid (Precirol ATO 5) in DCM at a 75:25 PLGA/Precirol ATO 5 mass ratio, along with 0.5% w/v Span 80 surfactant and 25 mg CUR. The internal water phase was emulsified with the oil phase using a Misonix Sonicator 3000 probe sonicator (QSonica, Newtown, CT) at an output power of 30 W for 30 s to form the primary W<sub>1</sub>/O emulsion. Then, 15 mL of aqueous surfactant solution (0.30% w/v PVA and 0.10% w/v SDBS) was poured into the W<sub>1</sub>/O emulsion and sonicated at an output power of 30 W for 30 s to produce a double W<sub>1</sub>/O/W<sub>2</sub> emulsion. This solution was stirred at a constant speed of 125 rpm for at least 4 h at 40 °C in order to remove DCM. The resulting suspension was centrifuged for three 20 min cycles and washed with DI water to remove any residual free drugs and surfactants. The average DOX/CUR ratio for the nanoparticles containing both drugs was equal to 5:1. This ratio was optimized in the preliminary in vitro experiments for the most effective killing of lung cancer cells. Janus particles containing DOX only were prepared using the protocol described above, except CUR was not included in the oil phase. Previous studies have shown that the amount of residual dichloromethane remaining in nanoparticles prepared using the solvent evaporation method is negligible (<15 ppm).<sup>29–31</sup> Guidelines established by USP 30 limit the acceptable amount of residual dichloromethane present in drug substance, excipients, and products to 600 ppm.<sup>32</sup> However, if there is a toxicity concern, a Class 3 solvent such as ethyl acetate can be used instead of dichloromethane. We have synthesized these particles using ethyl acetate as the organic solvent.

Janus particles containing CUR only were synthesized using a single oil-in-water emulsion template, as previously described.<sup>25</sup> A solution containing 2.5% w/v PLGA/Precirol ATO 5 and 25 mg of curcumin in DCM comprised the oil phase; 0.30% w/v PVA and 0.10% w/v SDBS aqueous solution was the water phase. The oil phase was added to the water phase and emulsified using sonication, followed by evaporation of the organic solvent.

For separate optical and fluorescent microscopic studies, larger microscale particles were used. For synthesis of these particles described above procedure was used. However, in this case, the two-phase mixture system was emulsified by manual agitation instead of sonication. Applying fewer shears resulted in significantly larger emulsion droplets and ultimately larger particles. The larger droplets required longer evaporation times, approximately 6 h on average.

#### Particle Size, Zeta Potential, Cytotoxicity and Genotoxicity.

The particle size distribution and zeta potential were measured by Malvern ZetaSizer NanoSeries (Malvern Instruments, U.K.) according to the manufacturer's instructions. All measurements were carried out at room temperature. Each parameter was measured five times for each batch, and average values and standard deviations were calculated. Laser diffraction was also used in addition to the ZetaSizer to measure particle size. Results obtained using laser diffraction were similar to those from proton correlation spectroscopy (PCS) and as such were not included in the manuscript to avoid repetition. Cytotoxicity of Janus nanoparticles (450 nm) was analyzed using a modified 3-(4,5-dimethylthiazol-2-yl)-(2,5-diphenyltetrazolium bromide) (MTT) assay within 24, 48, and 72 h as previously described.<sup>9</sup> Briefly, 10 000 A-549 human lung cancer cells were incubated separately in 96-well microtiter plate with different concentrations of empty Janus nanoparticles (2–20 mg/mL), free nonbound DOX (0.0003–0.65 mg/mL), Janus nanoparticles with CUR (0.0004–0.35 mg/mL), Janus nanoparticles with DOX (0.0002–1.75 mg/mL), Janus nanoparticles with CUR (0.0004–0.35 mg/mL), and DOX (0.0002–1.75 mg/mL). Different concentrations of particles were used to select a

noncytotoxic dose of nanoparticles that provide for survival of 100% cells. This concentration of nanoparticles was used in all future experiments with both drugs.

Genotoxicity of the studied particles were evaluated using the in vitro micronucleus assay as previously described.<sup>9</sup> Briefly, about 3000 cells were cultured with the media in 25 cm<sup>2</sup> flasks and held 24 h before treatment. They were then incubated with particles for 24, 48, and 72 h. Negative control cells were incubated with fresh media, while positive control cells were treated with 400 g/mL ethylmethanesulfonate—EMC (positive control). After incubation, the cells were fixed in a cold solution of 100% methanol. The methanol was removed and the cells were washed with phosphate buffer and cell nuclei were then stained with 600 nM of DAPI for 8 min. This solution was removed and all the flasks were washed with PBS containing 0.05% Tween 20. After staining, the formation of micronuclei was detected by a fluorescent microscope (Olympus, New York, NY) and documented by counting the number of micronuclei per 1000 cells.

**Synthesis of Labeled Polymer and Lipid.** FITC-labeled PLGA was synthesized via the carbodiimide method.<sup>33</sup> Briefly, 0.5 g PLGA was dissolved in 0.75 mL DCM. The carboxylate groups of PLGA were activated by the addition of 0.1 g NHS and 0.15 g N-(3-(Dimethylamino)propyl)-N'-ethylcarbodiimide to form PLGA-NHS. The reaction was stirred for 2 h. Separately, 0.6 g FITC was dissolved in 0.25 mL DCM and 0.25 mL pyridine. The FITC solution was added to the PLGA-NHS solution and stirred for 24 h, then quenched with 0.1 N HCl. The organic layer was extracted by DCM and washed with water. Following complete solvent evaporation, the solution was centrifuged for 20 min. The supernatant was discarded and the precipitate was washed with diethyl ether to obtain PLGA-FITC. The stained polymer was dried in a desiccator overnight and refrigerated until use.

Stock solution of a lipophilic tracer DiR was prepared by adding 4 mL DCM to the 0.01 g DiR (final concentration of 2.5 mg/mL). DiR-labeled Precirol was produced by first dissolving 0.5 g Precirol in 25 mL DCM. Next, 0.2 mL DiR solution was added to the lipid solution. The mixture was stirred overnight in a closed container. The DCM was then evaporated, leaving Precirol-DiR. The stained lipid was dried in a desiccator overnight and refrigerated for the further use.

**Confocal and Scanning Electron Microscopy.** Cellular internalization of Janus nanoparticles was monitored in A549 lung cancer cells by confocal microscopy as previously described.<sup>9,11,23</sup> Briefly, Polymeric (PLGA) phase of nanoparticle was labeled with FITC (green fluorescence), and lipid phase was labeled with DiR (red fluorescence). Cells were incubated with the particles for 24 h at 37 °C and red and green fluorescence images were photographed and digitally overlaid. Superimposition of images allows for detecting of colocalization of PLGA and lipid phases of nanoparticles (yellow color). Images observed by confocal microscopy (LSM 500; Carl Zeiss, Germany) using manufacturer image analyzer software.

Particle morphology was observed using a scanning electron microscope (SEM) type Amray 1830 I (SEMTech Solutions, North Billerica, MA). Samples were mounted onto metallic stabs with double-sided adhesive tape. Prior to imaging, samples were sputter coated with carbon using a Balzers SCD Sputter Coater.

**Animals.** Athymic nu/nu mice 6–8 weeks old were obtained from Taconic (Hudson, NY). All mice were maintained in microisolated cages under pathogen free conditions in the animal maintenance facilities of Rutgers, The State University of New Jersey. Veterinary care followed the guidelines described in the guide for the care and use of laboratory animals (AAALAC) as well as the requirements established by the animal protocol approved by the Rutgers Institutional Animal Care and Use Committee (IACUC).

**Inhalations Exposure System.** A one-jet Collison nebulizer (BGI Inc., Waltham, MA) operated at an aerosolization flow rate of 2 L/min using dry and purified air (Airgas East, Salem, NH) was used to aerosolize particles while an additional air flow of 2–3 L/min was introduced to dilute and desiccate the resulting aerosol according to the previously described procedure.<sup>10,11,23,34</sup> Briefly, the Collison nebulizer was equipped with a precious fluid cup to minimize the

amount of liquid needed for reliable aerosolization. Then, under slight positive pressure, the entire aerosol flow of 4–5 L/min entered a mixing box of the 5-port exposure chamber (CH Technologies, Westwood, NJ) and was distributed to each animal containment tube via round pipes (four out of five chambers were used in the experiments). Each containment tube was connected to the distribution chamber via a connector cone, which features a spout in its middle to deliver fresh aerosol to a test animal and round openings in its back for exhaled air. During the inhalation experiments, each tested animal was positioned in a containment tube so that the animal's nose was at the spout, or "inhalation point". The animal was held in place by a plunger. The air exhaled by the test animal escapes the connector cone via openings in the cone's back and was exhausted.

**Distribution of Janus Nanoparticles in Different Organs.** The distribution of Janus nanoparticles (155 and 450 nm) labeled with DiR was examined in nude mice after intravenous or inhalation administration as previously described.<sup>10,11,23</sup> Intravenously administered volume was 100  $\mu$ L for each formulation. For inhalation administration, the same volume (100  $\mu$ L) of suspension was used for each mouse. Our previous estimates showed that each mouse received about 1.2  $\mu$ g of the inhaled substance.<sup>34</sup> Each experimental group consisted of 6–10 mice. Animals were anesthetized with isoflurane and euthanized, 1 and 24 h after the treatment. Lungs, liver, spleen, heart, and kidneys were excised, rinsed in saline, and fluorescence was registered by IVIS imaging system (Xenogen Corporation, Alameda, CA). Images of each organ were scanned and total fluorescence intensity was calculated using the manufacturer software. The method allows a quantitative comparison of the concentration of the same fluorescent dye between different series of the experiments. The mass of all organs was measured and the fluorescence intensity was normalized by organ mass.

**Orthotopic Lung Cancer Model, Imaging, and Treatment.** A mouse orthotopic model of human lung cancer previously developed in our laboratory<sup>10,11,23</sup> was used in the current study. Briefly, A549 human lung adenocarcinoma epithelial cells ( $5\text{--}8 \times 10^6$ ) transfected with luciferase were resuspended in 0.1 mL of RPMI medium containing 20% fetal bovine serum, mixed with 5  $\mu$ L of EDTA and administered intratracheally to the lungs of athymic nu/nu mice through a catheter. The development of tumor was monitored and tumor volume was calculated using different imaging systems in live animals as previously described.<sup>10,11</sup> All imaging procedures were performed under inhalation anesthesia with isoflurane at a concentration of 4% for induction of anesthesia and 1–2% for maintenance. Mice were placed in prone position with isoflurane supplied via a nose cone. After the image data acquisition, the recovery time of the animals from anesthesia was usually less than 5 min. Optical imaging was performed using in vivo bioluminescent IVIS (Xenogen, Alameda, CA) and magnetic resonance imaging (MRI) was carried by 1TM2 whole body scanner (Aspect Imaging Shoham, Israel) systems as previously described.<sup>11</sup> In order to visualize cancer cells transfected with luciferase, luciferin was injected intraperitoneally in dose of 150 mg luciferin/kg of body weight 10–15 min before imaging. The treatment of animals started when the total volume of lung tumor reached approximately 50  $\text{mm}^3$  (4–6 weeks after inoculation of cancer cells). The following series of experiments were carried out: (1) Untreated mice (control); (2) mice treated by inhalation with empty Janus nanoparticles; (3) mice treated by intravenous (i.v.) injection with free nonbound DOX; (4) mice treated by inhalation with Janus nanoparticles loaded with CUR; (5) mice treated by inhalation with Janus nanoparticles loaded with DOX; and (6) mice treated by inhalation with Janus nanoparticles loaded with two drugs—DOX and CUR. The dose of both drugs in all drug-containing formulations was 2.5 mg/kg for the single administration. This dose corresponds to the maximum tolerated dose (MTD) estimated in separate experiments based on animal weight change after the instillation of increasing doses of drug formulation. The dose that led to the decrease of mouse body weight by 15% was considered as the MTD. The animals were treated twice per week within 4 weeks. Body weight of each mouse was measured using the electronic balances every second day.

**Statistical Analysis.** Data were analyzed using descriptive statistics, single-factor analysis of variance (ANOVA), and presented as mean values  $\pm$  the standard deviation (SD) from six to ten independent measurements. The comparison among groups was performed by the independent sample Student's test. The difference between variants is considered significant if  $P < 0.05$ .

## RESULTS

**Particles Characterizations.** Polymer/lipid Janus particles display an interesting and unique morphology (Figure 1). Specifically, these particles exhibited a longer, cone-shaped tail bound to a spherical polymer head ("ice cream cone" shape). Optical (Figure 1b), scanning electron (Figure 1c), and confocal (Figure 1d) microscope images showed clear phase separation of lipid/polymer particles. Ten batches of nanoparticles were produced and characterized. The size of nanoparticles used for in vitro and in vivo studies measured by different methods was  $155 \pm 10$  and  $450 \pm 23$  nm and characterized by a relatively narrow size distribution. The polydispersity index (PDI) was  $0.29 \pm 0.08$  and  $0.33 \pm 0.18$ , respectively for smaller and larger nanoparticles, respectively (means  $\pm$  S.D.). Figure 2 shows an example of size distribution

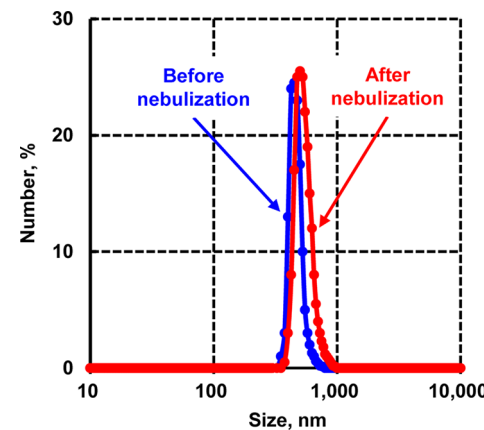


**Figure 2.** Size distribution of 450 nm Janus nanoparticles before and after nebulization. These particles were used for in vivo treatment of animals by inhalation. A representative size distribution pattern is shown.

of 450 nm nanoparticles before and after nebulization that were used for in vivo treatment of animals by inhalation. The average surface charge (zeta potential) of PLGA/Precirol nanoparticles was equal to  $-15.22 \pm 1.78$  mV (means  $\pm$  S.D.).

**Cytotoxicity and Genotoxicity.** Cytotoxicity of Janus nanoparticles was analyzed by a modified MTT assay (Figure 3a). The results indicated that empty nanoparticles did not affect viability of lung cancer cells in all studied concentrations. Further experiments did not show any signs of genotoxicity of these nanoparticles. We found that incubation of cells with empty Janus nanoparticles did not induce the formation of micro nuclei (Figure 3b,c). As expected, free nonbound DOX induced cell death in cancer cells and therefore cellular viability was decreased (Figure 3a). It should be noted that due to the very poor water solubility of CUR it was impossible to measure cell viability with the free nonbound drug. Binding of DOX to nanoparticles slightly but statistically significant ( $P < 0.05$  when compared with free drug) enhanced its cytotoxicity. In contrast to DOX-loaded nanoparticles, CUR containing particles demonstrated considerably lower cytotoxicity in lung cancer

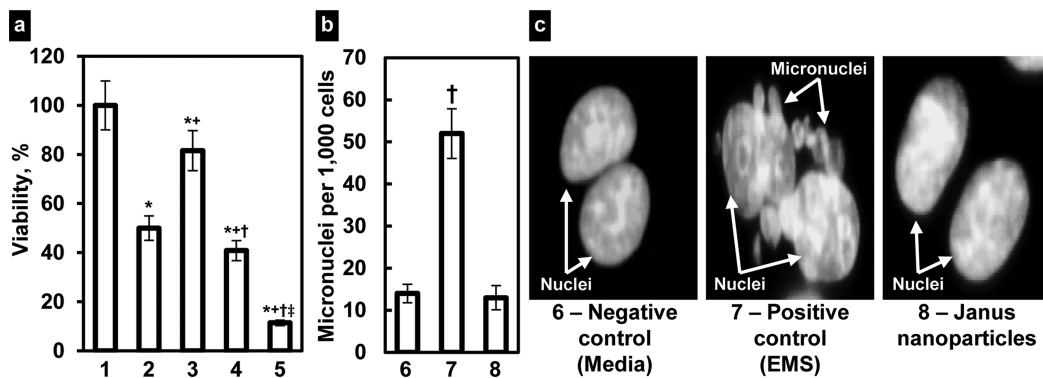


**Figure 3.** Cyto- and genotoxicity of studied substances. (a) Viability of A549 human lung cancer cells. Cells were incubated within 24 h with following formulations: 1, Empty Janus nanoparticles, 2, Free nonbound DOX, 3, Janus nanoparticles with CUR, 4, Janus nanoparticles with DOX, 5, Janus nanoparticles with CUR and DOX. (b, c) Genotoxicity (formation of micronuclei) of Janus nanoparticles and corresponding controls. (b) Quantitative analysis of micronuclei formation. (c) Representative fluorescence microscopy images of cell incubated within 24 h with 6, Media (negative control), 7, EMS (positive control, and 8, Janus nanoparticles. Means  $\pm$  SD are shown. \* $P < 0.05$  when compared with empty nanoparticles; † $P < 0.05$  when compared with free DOX; ‡ $P < 0.05$  when compared with nanoparticles with CUR; and ‡‡ $P < 0.05$  when compared with nanoparticles with DOX.

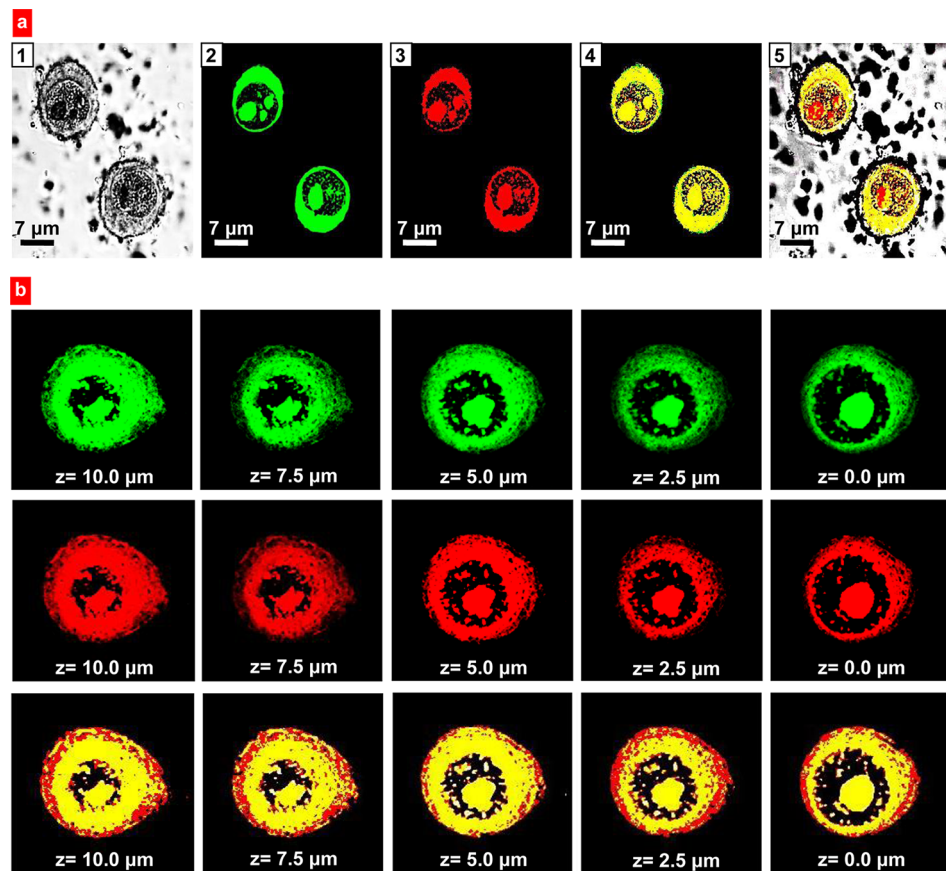


**Figure 4.** Intracellular localization of anisotropic biodegradable polymer/lipid Janus nanoparticles. (a) Representative images of A549 human lung cancer cells incubated 24 h with nanoparticles: 1, Light; 2–4, Fluorescence; 2, Polymeric (PLGA) phase of nanoparticles was labeled with FITC (green fluorescence); 3, Lipid (precirol) phase was labeled with DiR (red fluorescence); 4, Superimposition of green and red fluorescence images shows colocalization of PLGA and lipid phases of nanoparticles (yellow color); and 5, Superimposition of light, green and red fluorescence images shows intracellular localization of nanoparticles. (b) Representative confocal microscopy (z-series, from the top of the cell to the bottom) images of A549 human lung cancer cells incubated for 24 h with anisotropic biodegradable polymer/lipid Janus nanoparticles. Polymeric (PLGA) phase of nanoparticles was labeled with FITC (green fluorescence); lipid (precirol) phase was labeled with DiR (red fluorescence). Superimposition of green and red fluorescence images shows colocalization of PLGA and lipid phases of nanoparticles (yellow color).

cells. However, the decrease in cell viability after the incubation with CUR-loaded nanoparticles was statistically more pronounced ( $P < 0.05$ ) when compared with empty nanoparticles.

It should be stressed that the incubation of cells with the combination of two anticancer drugs with different mechanisms of action and solubility loaded into Janus nanoparticles

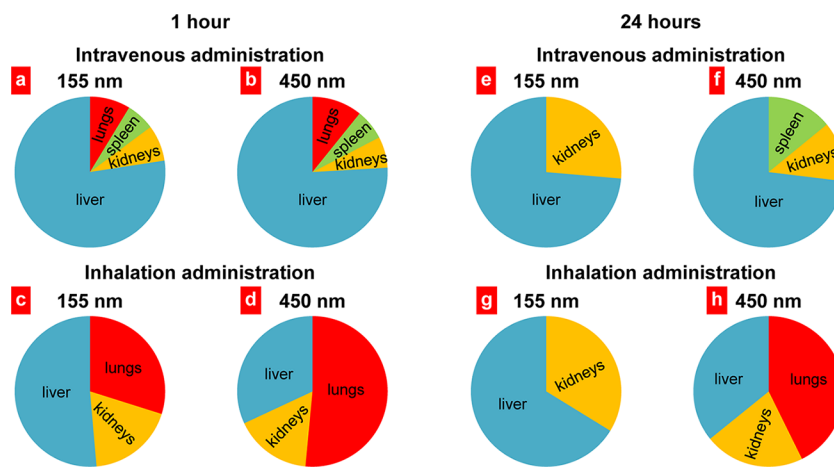


**Figure 5.** Distribution of anisotropic biodegradable polymer/lipid Janus nanoparticles in different organs 1 and 24 h after intravenous or inhalation administrations. Mean values for eight animals are presented.

demonstrated their synergistic effect. In fact, the viability of lung cancer cells decreased approximately in 5 times after their incubation with nanoparticles containing both drugs (Figure 3 a). This decrease in cell viability was statistically significant ( $P < 0.05$ ) when compared both drug-nanoparticle formulations with empty nanoparticles, free DOX, and nanoparticles containing just one drug. It should be stressed that empty nanoparticles did not show any signs of cyto- and genotoxicity within all studied periods (24, 48, and 72 h).

**Cellular Internalization.** Cellular internalization of Janus nanoparticles was evaluated using confocal microscopy. A-549 human lung carcinoma cells were incubated with particles labeled simultaneously with two fluorescent dyes: FITC (polymeric phase of particles) and DiR (lipid phase of nanoparticles) (Figure 4a, b). The results revealed that after 24 h of incubation, a substantial amount of Janus nanoparticles was detected in both cellular plasma and nucleus (Figure 4a). In order to demonstrate that nanoparticles were not adhered to the cellular surface and penetrated into the cells, we analyzed their distribution in different cellular layers from the top of the cells to the bottom of the cells (z-sections, Figure 4b). The data showed that intracellular distribution of Janus nanoparticles was very similar in different cell layers. Hence, the developed anisotropic carriers can potentially be used for administration of therapeutic agents with different solubility and preferential biological activity both in the cellular cytoplasm and nuclei.

**Body Distribution.** A Collison nebulizer connected to four-port, nose-only exposure chambers was used for inhalation delivery of drug-loaded nanoparticles. The measurement of nanoparticle size showed that nebulization did not influence significantly on the size and stability of nanoparticles (Figure 2). The results presented on Figure 5 revealed that 1 h after intravenous administration the distribution patterns of 155 nm (Figure 5a) and 450 nm (Figure 5b) Janus nanoparticles were similar to the preferential particle accumulation in mouse liver. However, slightly higher accumulation in the lungs was found for the larger nanoparticles. One hour after inhalation delivery, nanoparticles of both sizes were detected in the lungs (Figure 5c,d); however, the accumulation of nanoparticles with 450 nm in diameter was twice higher when compared with 155 nm nanoparticles. The analysis of the distribution profile of Janus nanoparticles 24 h after their intravenous administrations showed that the majority of nanoparticles of both sizes were found in the liver and kidneys, while no fluorescent signal was

detected in lungs (Figure 5e,f). As was mentioned above, the accumulation of larger nanoparticles in the lungs 1 h after treatment was substantially higher when compared with smaller nanoparticles (Figure 5c,d). However, 24 h after inhalation, similarly to the intravenous administration, the 155 nm nanoparticles were found only in the liver and kidneys (Figure 5g). In contrast, larger nanoparticles were still detected in the lungs 24 h after inhalation and their content was comparable with that after 1 h after treatment (Figure 5d, h). On the basis of these results we selected Janus nanoparticles with the size of 450 nm for further inhalation treatment of mice with orthotopic lung cancer.

**Lung Cancer Treatment.** To create an orthotopic murine model of lung cancer, A549 human lung cancer cells were transfected with luciferase and injected intratracheally into the lungs of nude mice. The initial deposition of cancer cells in the lungs and the subsequent progression of the lung tumor were analyzed using different imaging systems (measuring the bioluminescence of transfected cancer cells by IVIS and MRI (Figure 6a,b) in live, anesthetized animals. After the tumor volume reached the size of approximately  $50 \text{ mm}^3$ , mice were treated twice per week during 4 weeks by inhalation with different drug formulations of Janus nanoparticles (450 nm). The following series of treatments were carried out: (1) Untreated animals (control); (2) Inhalation treatment with empty nanoparticles; (3) Intravenous treatment with free nonbound doxorubicin; (4) Inhalation treatment with nanoparticles containing curcumin; (5) Inhalation treatment with nanoparticles containing doxorubicin; and (6) Inhalation treatment with nanoparticles containing curcumin and doxorubicin. Inhalation of mice with empty nanoparticles did not influence significantly on the size of lung tumor. In contrast, all types of inhalation treatment with nanoparticles containing drug(s) led to a substantial limitation of tumor progression (Figure 6c). Consistent with cytotoxicity data, nanoparticles loaded with DOX were more effective in terms of the suppression of tumor growth when compared with nanoparticles loaded with CUR. It should be noted that the concentrations of both drugs in all particle formulations used for the *in vivo* study was equal to 2.5 mg/kg for a single administration. In contrast, intravenous administration of free DOX only slightly suppressed tumor progression. However, the highest antitumor effect was achieved after inhalation with the nanoparticles simultaneously loaded with both drugs. This type

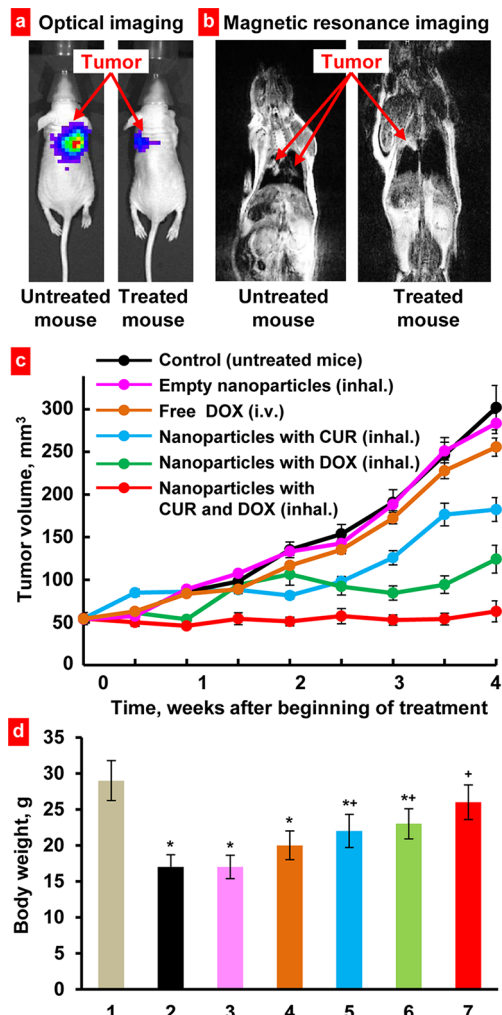


**Figure 6.** Suppression of lung tumor growth in mice inhaled with Janus nanoparticles containing anticancer drug(s). Representative optical (a) and magnetic resonance (b) images 4 weeks after tumor instillation. (c) Changes in lung tumor volume after beginning of treatment. (d) Body weight of mice at the end of experiment. (1), Healthy mice without tumor; (2), Untreated mice with tumor; (3–7), Mice with tumor treated with empty nanoparticles; (3), free DOX (4), nanoparticles with CUR (5), nanoparticles with DOX (6), and nanoparticles with CUR and DOX (7). \* $P < 0.05$  when compared with healthy mice without tumor. \*\* $P < 0.05$  when compared with untreated mice with tumor. The treatment of animals started when the total volume of lung tumor reached approximately  $50 \text{ mm}^3$  (4–6 weeks after inoculation of cancer cells). Mice were treated twice per week within 4 weeks. Means  $\pm$  SD ( $n = 10$ ) are shown.

of treatment almost completely prevented the progression of tumor. The measurements of body weight showed that the weight of untreated animals with tumor was significantly ( $P < 0.05$ ) lower when compared with healthy mice without tumor (Figure 6d). Treatment with free DOX and nanoparticles with only one drug (CUR or DOX) partially prevent the weight loss. Combinatorial inhalation treatment with both drugs almost completely restored mouse weight ( $P > 0.05$  when compared with healthy mice without tumor).

## DISCUSSION

The presented study is aimed at developing and characterizing the biodegradable polymer/lipid anisotropic Janus nanoparticles in order to evaluate them as a potential drug delivery

system for the treatment of lung cancer. The novel anisotropic particles were grown and self-assembled in large-batch, scalable, single-pot synthesis using a modified double emulsion-solvent evaporation technique. The primary advantage of the proposed particles is the presence of less and more hydrophilic parts in one particle simultaneously which allows for effective simultaneous loading of hydrophilic and lipophilic drugs. Such a strategy could be beneficial in treating many types of cancer that develop resistance to the same chemotherapeutic agent administered over time. It also may help in the use of two biologically active agents with different mechanism of action and synergism in treatment of different diseases including lung cancer. The synthesized nanoparticles had an “ice cream cone” like structure. Previously, we observed phase segregation of Precirol and PLGA or PCL into formation of such structures.<sup>25</sup> The formation behavior of these particles was entirely different in nature than that of the polymer/polymer particles. Rather than slow particle segregation analogous to cell division, the lipid Precirol “cone” precipitated long before the polymer component. Supersaturation of the lipid was reached much faster than that of the polymer, despite the lipid being present at significantly lower levels (25 wt % compared to 75 wt % of polymer). The lipid tail remained at the interface of the droplet as the spherical polymer component was formed.

During the study, we found that biodegradable Janus nanoparticles alone (without any drugs) did not demonstrate toxicity and did not induce formation of micro nuclei. Consequently, the synthesized nanoparticles themselves were neither cytotoxic nor genotoxic. These findings support the assumption that being injected systemically to the body Janus nanocarriers potentially would not produce additional toxic effect on organs and tissues during their degradation. The absence of cytotoxic effects makes these Janus nanoparticles an ideal candidate for the delivery of different drugs for treating various diseases in addition to cancer.

In vitro studies showed that the PLGA/Precirol Janus particles do not affect cell viability. Furthermore, when broken down to its individual components, the biodegradability of Janus particles is confirmed. PLGA is an FDA-approved, biodegradable polymer frequently used in drug delivery.<sup>35–37</sup> Precirol ATO 5 is an FDA-approved lipid frequently used in the production of solid lipid nanoparticles for drug delivery.<sup>38</sup> The surfactants PVA and SDDBS are theoretically removed in the washing step. Although 100% removal is not possible, previous studies show that the amount of residual PVA associated with PLGA nanoparticles is proportional to the concentration of PVA used in the external aqueous phase.<sup>39</sup> For example, 0.5% w/v initial PVA concentration results in approximately 2% w/w residual PVA; whereas 5% w/v starting concentration resulted in approximately 5% w/w residual PVA. For the present study, a relatively low concentration of surfactant was used (0.4% w/v). PVA is considered a biodegradable polymer and is approved by the FDA for clinical use.<sup>40,41</sup> SDDBS is also biodegradable.<sup>42</sup> Consequently, one can consider the nanoparticles synthesized in the present study as biodegradable.

The next step in our study was dedicated to demonstrating that developed anisotropic carriers can penetrate lung cancer cells and release their active payloads providing a multipronged attack thus causing a more effective killing of the cells. The obtained results confirmed our hypothesis and showed that studied dual hydrophilic/hydrophobic nanoparticles were capable to penetrate the cells and successfully deliver their active components destroying almost 90% of cancer cells. It was

also found that nanoparticles accumulate inside cells both in the cytoplasm and nuclei. This, in turn, allows for delivering drugs with cytoplasmic and nuclear mechanisms of action.

In order to proceed with the lung cancer treatment, the nanoparticles were nebulized and delivered into the mouse lungs by inhalation using the nose-only exposure chambers. The labeling of nanoparticles with a fluorescent dye allowed for studying the distribution profile of Janus particles with different sizes was studied. In particular, their ability to accumulate in the lungs of experimental animals after intravenous and inhalation administrations was analyzed. It was found that the combination of two important factors: size and route of administration, played the critical role in the Janus particles distribution profile. Particles with the diameter of 450 nm showed the highest accumulation and longest retention on the lungs after their inhalation delivery. The smallest particles probably faster penetrated into the bloodstream through alveoli-capillary barrier and therefore may be less effective in the treatment of lung diseases by inhalation and could potentially induce adverse side effects of treatment on healthy tissues. The retention of the nanoparticles in the lungs was studied within 24 h because it is known that all material which accumulates in the lungs is removed in about 24 h because of the cephalad movement of the mucus blanket.<sup>43</sup> The body distribution of Janus nanoparticles after inhalation is very similar to other types of particles with comparable sizes. In fact, liposomes, nanostructured lipid carriers and mesoporous silica nanoparticles with the size of 300–500 nm preferentially accumulated in the lungs after their administration by inhalation.<sup>10,11,23,44–46</sup>

Thus, for further *in vivo* experiments in order to enhance the efficiency of cancer treatment and minimize adverse side effects of particles loaded with highly toxic anticancer drugs we proposed of using 450 nm nanoparticles and employing the local pulmonary route of administration by inhalation.

The selected nanoparticles loaded with doxorubicin and curcumin were tested using orthotopic murine model of human lung cancer. Intravenous injection of free nonbound doxorubicin was used as a model of currently used in clinic chemotherapeutic treatment protocol. Obtained results clearly demonstrated that local inhalation treatment of mice bearing lung tumors using Janus nanoparticles loaded with two anticancer drugs were able to successfully suppress the tumor growth. In contrast, the treatment of mice with free doxorubicin injected intravenously only slightly limited the growth of lung tumor. This result confirms the fact that simultaneous use of two drugs with different aqueous solubility and mechanisms of action is very beneficial for the success of cancer treatment. We also confirmed the synergism of these two drugs in accomplishing such high antitumor effect that cannot be achieved by treating the mice with the Janus particles containing only one drug. Consequently, dual chemotherapy with the proposed anisotropic Janus nanoparticles can be beneficial for treating of cancers that are resistant to the one particular drug or in enhancing the antitumor efficacy of an anticancer drug by coencapsulation with another drug or biologically active agent with synergistic effect. In the present study, we used doxorubicin and curcumin as model anticancer drugs in a proof-of-concept study. However, we cannot foresee obstacles for encapsulating any types of hydrophilic and hydrophobic drugs.

## CONCLUSIONS

The proposed anisotropic Janus nanoparticles have a high potential for the delivery of drugs with different physicochemical properties and can be used in chemotherapy of various types of cancers and treating other diseases. In particular, the present study confirmed their exceptional efficiency in local inhalation codelivery of hydrophilic and hydrophobic anti-cancer drugs and limiting the progression of lung cancer.

## AUTHOR INFORMATION

### Corresponding Authors

\*Phone: 732-445-2972; fax: 732-445-2581; e-mail: silvina@sol.rutgers.edu.

\*Phone: 848-445-6348; fax: 732-445-3134; e-mail: minko@rci.rutgers.edu.

### Author Contributions

<sup>§</sup>These authors contributed equally to this work.

### Notes

The authors declare no competing financial interest.

## ACKNOWLEDGMENTS

The work was supported in part by R01 grants CA111766 and HL118312 from the National Institutes of Health. We thank Dr. D. C. Reimer and Mr. V. Starovoytov for their help with the development and implementation of orthotopic mouse model of lung cancer and obtaining and providing analysis of transmission electron microscopy images, respectively.

## REFERENCES

- (1) Haley, B.; Frenkel, E. Nanoparticles for drug delivery in cancer treatment. *Urol. Oncol.* **2008**, *26*, 57–64.
- (2) Matsumura, Y. The drug discovery by nanomedicine and its clinical experience. *Jpn. J. Clin. Oncol.* **2014**, *44*, 515–525.
- (3) Moghimi, S. M. Cancer nanomedicine and the complement system activation paradigm: Anaphylaxis and tumour growth. *J. Controlled Release* **2014**, *190*, 556–562.
- (4) Saadeh, Y.; Leung, T.; Vyas, A.; Chaturvedi, L. S.; Perumal, O.; Vyas, D. Applications of nanomedicine in breast cancer detection, imaging, and therapy. *J. Nanosci. Nanotechnol.* **2014**, *14*, 913–923.
- (5) Drbohlavova, J.; Chomoucka, J.; Adam, V.; Ryvolova, M.; Eckschlager, T.; Hubalek, J.; Kizek, R. Nanocarriers for anticancer drugs—New trends in nanomedicine. *Curr. Drug Metab.* **2013**, *14*, 547–564.
- (6) Rizzo, L. Y.; Theek, B.; Storm, G.; Kiessling, F.; Lammers, T. Recent progress in nanomedicine: Therapeutic, diagnostic and theranostic applications. *Curr. Opin Biotechnol.* **2013**, *24*, 1159–1166.
- (7) Etheridge, M. L.; Campbell, S. A.; Erdman, A. G.; Haynes, C. L.; Wolf, S. M.; McCullough, J. The big picture on nanomedicine: the state of investigational and approved nanomedicine products. *Nanomed.: Nanotechnol., Biol., Med.* **2013**, *9*, 1–14.
- (8) Mitra, A.; Nan, A.; Line, B. R.; Ghandehari, H. Nanocarriers for nuclear imaging and radiotherapy of cancer. *Curr. Pharm. Des* **2006**, *12*, 4729–4749.
- (9) Shah, V.; Taratula, O.; Garbuzenko, O. B.; Patil, M. L.; Savla, R.; Zhang, M.; Minko, T. Genotoxicity of different nanocarriers: Possible modifications for the delivery of nucleic acids. *Curr. Drug Discov. Technol.* **2013**, *10*, 8–15.
- (10) Garbuzenko, O. B.; Saad, M.; Pozharov, V. P.; Reuhl, K. R.; Mainelis, G.; Minko, T. Inhibition of lung tumor growth by complex pulmonary delivery of drugs with oligonucleotides as suppressors of cellular resistance. *Proc. Natl. Acad. Sci. U. S. A.* **2010**, *107*, 10737–10742.
- (11) Taratula, O.; Kuzmov, A.; Shah, M.; Garbuzenko, O. B.; Minko, T. Nanostructured lipid carriers as multifunctional nanomedicine

- platform for pulmonary co-delivery of anticancer drugs and siRNA. *J. Controlled Release* **2013**, *171*, 349–357.
- (12) Mussi, S. V.; Sawant, R.; Perche, F.; Oliveira, M. C.; Azevedo, R. B.; Ferreira, L. A.; Torchilin, V. P. Novel nanostructured lipid carrier co-loaded with doxorubicin and docosahexaenoic acid demonstrates enhanced in vitro activity and overcomes drug resistance in MCF-7/Adr cells. *Pharm. Res.* **2014**, *8*, 1882–1892.
- (13) Wang, T.; Hartner, W. C.; Gillespie, J. W.; Praveen, K. P.; Yang, S.; Mei, L. A.; Petrenko, V. A.; Torchilin, V. P. Enhanced tumor delivery and antitumor activity in vivo of liposomal doxorubicin modified with MCF-7-specific phage fusion protein. *Nanomed.: Nanotechnol., Biol., Med.* **2014**, *10*, 421–430.
- (14) Tong, S. W.; Xiang, B.; Dong, D. W.; Qi, X. R. Enhanced antitumor efficacy and decreased toxicity by self-associated docetaxel in phospholipid-based micelles. *Int. J. Pharm.* **2012**, *434*, 413–419.
- (15) Zhao, B. J.; Ke, X. Y.; Huang, Y.; Chen, X. M.; Zhao, X.; Zhao, B. X.; Lu, W. L.; Lou, J. N.; Zhang, X.; Zhang, Q. The antiangiogenic efficacy of NGR-modified PEG-DSPE micelles containing paclitaxel (NGR-M-PTX) for the treatment of glioma in rats. *J. Drug Target* **2011**, *19*, 382–390.
- (16) Abouzeid, A. H.; Patel, N. R.; Rachman, I. M.; Senn, S.; Torchilin, V. P. Anti-cancer activity of anti-GLUT1 antibody-targeted polymeric micelles co-loaded with curcumin and doxorubicin. *J. Drug Target* **2013**, *21*, 994–1000.
- (17) Sawant, R. R.; Jhaveri, A. M.; Koshkaryev, A.; Qureshi, F.; Torchilin, V. P. The effect of dual ligand-targeted micelles on the delivery and efficacy of poorly soluble drug for cancer therapy. *J. Drug Target* **2013**, *21*, 630–638.
- (18) Shcharbin, D.; Shakhbazau, A.; Bryszewska, M. Poly-(amidoamine) dendrimer complexes as a platform for gene delivery. *Exp. Opin. Drug Deliv.* **2013**, *10*, 1687–1698.
- (19) Mignani, S.; El Kazzouli, S.; Bousmina, M.; Majoral, J. P. Expand classical drug administration ways by emerging routes using dendrimer drug delivery systems: a concise overview. *Adv. Drug Deliv Rev.* **2013**, *65*, 1316–1330.
- (20) Najlah, M.; D'Emanuele, A. Synthesis of dendrimers and drug-dendrimer conjugates for drug delivery. *Curr. Opin. Drug Discov. Devel.* **2007**, *10*, 756–767.
- (21) Neerman, M. F.; Zhang, W.; Parrish, A. R.; Simanek, E. E. In vitro and in vivo evaluation of a melamine dendrimer as a vehicle for drug delivery. *Int. J. Pharm.* **2004**, *281*, 129–132.
- (22) He, Q.; Shi, J. MSN anti-cancer nanomedicines: Chemotherapy enhancement, overcoming of drug resistance, and metastasis inhibition. *Adv. Mater.* **2014**, *26*, 391–411.
- (23) Taratula, O.; Garбуzenko, O. B.; Chen, A. M.; Minko, T. Innovative strategy for treatment of lung cancer: targeted nanotechnology-based inhalation co-delivery of anticancer drugs and siRNA. *J. Drug Target* **2011**, *19*, 900–914.
- (24) Perro, A.; Reculosa, S.; Ravaine, S.; Bourgeat-Lami, E.; Duguet, E. Design and synthesis of Janus micro- and nanoparticles. *J. Mater. Chem.* **2005**, *15*, 3745–3760.
- (25) Romanski, F. S.; Winkler, J. S.; Riccobene, R. C.; Tomassone, M. S. Production and characterization of anisotropic particles from biodegradable materials. *Langmuir* **2012**, *28*, 3756–3765.
- (26) Yoo, J. W.; Doshi, N.; Mitragotri, S. Adaptive micro and nanoparticles: Temporal control over carrier properties to facilitate drug delivery. *Adv. Drug Deliv Rev.* **2011**, *63*, 1247–1256.
- (27) Champion, J. A.; Mitragotri, S. Role of target geometry in phagocytosis. *Proc. Natl. Acad. Sci. U. S. A.* **2006**, *103*, 4930–4934.
- (28) Tomasini, M. D.; Zablocki, K.; Petersen, L. K.; Moghe, P. V.; Tomassone, M. S. Coarse grained molecular dynamics of engineered macromolecules for the inhibition of oxidized low-density lipoprotein uptake by macrophage scavenger receptors. *Biomacromolecules* **2013**, *14*, 2499–2509.
- (29) Mainardes, R. M.; Evangelista, R. C. PLGA nanoparticles containing praziquantel: Effect of formulation variables on size distribution. *Int. J. Pharm.* **2005**, *290*, 137–144.
- (30) Niwa, T.; Takeuchi, H.; Hino, T.; Kunou, N.; Kawashima, Y. In vitro drug release behavior of D,L-lactide/glycolide copolymer (PLGA) nanospheres with nafarelin acetate prepared by a novel spontaneous emulsification solvent diffusion method. *J. Pharm. Sci.* **1994**, *83*, 727–732.
- (31) Ubrich, N.; Bouillot, P.; Pellerin, C.; Hoffman, M.; Maincent, P. Preparation and characterization of propranolol hydrochloride nanoparticles: A comparative study. *J. Controlled Release* **2004**, *97*, 291–300.
- (32) Convention, U. S. P. USP 30; United States Pharmacopeial Convention, 2006.
- (33) Basu, S.; Harfouche, R.; Soni, S.; Chimote, G.; Mashelkar, R. A.; Sengupta, S. Nanoparticle-mediated targeting of MAPK signaling predisposes tumor to chemotherapy. *Proc. Natl. Acad. Sci. U. S. A.* **2009**, *106*, 7957–7961.
- (34) Mainelis, G.; Seshadri, S.; Garbuzenko, O. B.; Han, T.; Wang, Z.; Minko, T. Characterization and application of a nose-only exposure chamber for inhalation delivery of liposomal drugs and nucleic acids to mice. *J. Aerosol Med. Pulm. Drug Deliv.* **2013**, *26*, 345–354.
- (35) Kumari, A.; Yadav, S. K.; Yadav, S. C. Biodegradable polymeric nanoparticles based drug delivery systems. *Colloids Surf., B* **2010**, *75*, 1–18.
- (36) Makadia, H. K.; Siegel, S. J. Poly Lactic-co-glycolic acid (PLGA) as biodegradable controlled drug delivery carrier. *Polymers* **2011**, *3*, 1377–1397.
- (37) Sonaje, K.; Italia, J. L.; Sharma, G.; Bhardwaj, V.; Tikoo, K.; Kumar, M. N. V. R. Development of biodegradable nanoparticles for oral delivery of ellagic acid and evaluation of their antioxidant efficacy against cyclosporine A-induced nephrotoxicity in rats. *Pharm. Res.* **2007**, *24*, 899–908.
- (38) Gao, Z. H.; Crowley, W. R.; Shukla, A. J.; Johnson, J. R.; Reger, J. F. Controlled release of contraceptive steroids from biodegradable and injectable gel formulations: in vivo evaluation. *Pharm. Res.* **1995**, *12*, 864–868.
- (39) Sahoo, S. K.; Panyam, J.; Prabha, S.; Labhasetwar, V. Residual polyvinyl alcohol associated with poly (D,L-lactide-co-glycolide) nanoparticles affects their physical properties and cellular uptake. *J. Controlled Release* **2002**, *82*, 105–114.
- (40) Chong, S. F.; Smith, A. A.; Zelikin, A. N. Microstructured, functional PVA hydrogels through bioconjugation with oligopeptides under physiological conditions. *Small* **2013**, *9*, 942–950.
- (41) Matsumura, S.; Toshima, K. biodegradation of poly(vinyl alcohol) and vinyl alcohol block as biodegradable segment. In *Hydrogels and Biodegradable Polymers for Bioapplications*; American Chemical Society: Washington, D.C., 1996; Vol. 627, pp 137–148.
- (42) Manousaki, E.; Psillakis, E.; Kalogerakis, N.; Mantzavinos, D. Degradation of sodium dodecylbenzene sulfonate in water by ultrasonic irradiation. *Water Res.* **2004**, *38*, 3751–3759.
- (43) Minko, T. Drug delivery systems. In *Martin's Physical Pharmacy and Pharmaceutical Sciences*, Sed.; Sinko, P., Ed.; Lippincott Williams and Wilkins: New York, 2006; pp 629–680.
- (44) Garbuzenko, O. B.; Mainelis, G.; Taratula, O.; Minko, T. Inhalation treatment of lung cancer: The influence of composition, size and shape of nanocarriers on their lung accumulation and retention. *Cancer Biol. Med.* **2014**, *11*, 44–55.
- (45) Garbuzenko, O. B.; Saad, M.; Betigeri, S.; Zhang, M.; Vetcher, A. A.; Soldatenkov, V. A.; Reimer, D. C.; Pozharov, V. P.; Minko, T. Intratracheal versus intravenous liposomal delivery of siRNA, antisense oligonucleotides and anticancer drug. *Pharm. Res.* **2009**, *26*, 382–394.
- (46) Ivanova, V.; Garbuzenko, O. B.; Reuhl, K. R.; Reimer, D. C.; Pozharov, V. P.; Minko, T. Inhalation treatment of pulmonary fibrosis by liposomal prostaglandin E2. *Eur. J. Pharm. Biopharm.* **2013**, *84*, 335–344.